Journal of Organometallic Chemistry 696 (2011) 2993–2999

Contents lists available at ScienceDirect

Journal of Organometallic Chemistry

journal homepage: www.elsevier.com/locate/jorganchem

Syntheses and structural analysis of the sterically encumbered germanes (*o*-Bu^{t}C$_6$H$_4$)$_3$GeX (X = Br, H, Cl, OH), (*o*-Bu^{t}C$_6$H$_4$)$_2$GeBr$_2$, and Mes$_2$GeH$_2$: distortions arising from the presence of an *ortho-tert*-butyl substituent

Christian R. Samanamu [a], Courtney R. Anderson [a], James A. Golen [b,c], Curtis E. Moore [b], Arnold L. Rheingold [b], Charles S. Weinert [a,*]

[a] Department of Chemistry, Oklahoma State University, Stillwater, Oklahoma 74078, USA
[b] Department of Chemistry and Biochemistry, University of California San Diego, La Jolla, California 92093-0358, USA
[c] Department of Chemistry and Biochemistry, University of Massachusetts Dartmouth, North Dartmouth, Massachusetts 02747, USA

ARTICLE INFO

Article history:
Received 20 April 2011
Received in revised form
19 May 2011
Accepted 20 May 2011

Keywords:
Germanium
Chirality
Structural distortions
X-ray crystal structures

ABSTRACT

Four new *ortho-tert*-butylphenyl substituted germanes (*o*-Bu^{t}C$_6$H$_4$)$_3$GeX (X = Br (**1**), H (**2**), Cl (**3**), or OH (**4**)) have been prepared and structurally characterized. The structures of **1**–**4** have been obtained and the *ortho-tert*-butyl substituents were found to be oriented in the same direction as the Ge–X bond in each molecule. The presence of these bulky substituents results in distortions in **1**–**4** from the ideal tetrahedral geometry, which was assessed by an examination of the C$_{ipso}$–Ge–C$_{ipso}$–C$_{ortho}$ torsion angles within these four compounds. The two diaryl-substituted germanes (*o*-Bu^{t}C$_6$H$_4$)$_2$GeBr$_2$ (**5**) and Mes$_2$GeH$_2$ (**6**) have also been prepared and structurally characterized, and the absence of a third sterically encumbering aryl group alleviates a significant amount of structural strain in these compounds versus their triaryl-substituted analogues.

© 2011 Elsevier B.V. All rights reserved.

1. Introduction

We have utilized triarylgermanium hydrides and amides for the construction of germanium–germanium single bonds via the hydrogermolysis reaction (Scheme 1) [1–8] and were interested in the implementation of tri(*ortho-tert*-butyl)-substituted germanium halides and hydrides to function as possible chiral synthetic precursors. Although these systems do not contain an asymmetric carbon, they do exist as non-superimposable mirror images (Fig. 1) due to the restricted rotation about the Ge–C$_{ipso}$ bonds enforced by the *ortho-tert*-butyl groups, thus rendering these molecules chiral. However, compounds of this type having a high degree of steric encumbrance at the germanium center have been found to exhibit limited reactivity.

The structures of these tri(*ortho-tert*-butyl)-substituted germanium compounds are themselves of interest, as the presence of the bulky *ortho*-substituents can result in significant distortions of the ideal positions of the aryl rings relative to unsubstituted phenyl derivatives. In the ideal geometric case, the six *ortho*-carbons of the three aryl rings would all be co-planar, and would be lying in a plane that was disposed slightly beyond the plane defined by the three *ipso* carbon atoms. However, this ideal geometry is seldom realized in triarylgermanium compounds, and even the sterically unemcumbered species Ph$_3$GeH [9] is distorted from this ideal geometry and adopts a propeller-like structure by rotation of the aryl rings about the Ge–C$_{ipso}$ axis. The degree of steric interactions between the *ortho*-substituents of the three aryl rings are dependent on the size of the *ortho*-substituents present.

We have synthesized the germane (*o*-Bu^{t}C$_6$H$_4$)$_3$GeBr (**1**) and have converted this species to the three additional sterically encumbered germanes (*o*-Bu^{t}C$_6$H$_4$)$_3$GeX (X = H (**2**), Cl (**3**), OH (**4**)). We could not convert any of these four species to the desired amide compound (*o*-Bu^{t}C$_6$H$_4$)$_3$GeNMe$_2$ for use in the hydrogermolysis reaction. However, we have obtained the X-ray crystal structures of **1**–**4** and have assessed the degree of structural distortion in these molecules resulting from the presence of the three *ortho-tert*-butyl groups. The structures of **1**–**4** are also compared to those of several other related molecules. In addition, we have obtained the X-ray structures of the two diaryl-substituted species (*o*-Bu^{t}C$_6$H$_4$)$_2$GeBr$_2$ (**5**) and Mes$_2$GeH$_2$ (**6**) [10] which are also compared to the structures of their corresponding triaryl-substituted analogues.

* Corresponding author. Tel.: +1 405 744 6543.
E-mail address: weinert@chem.okstate.edu (C.S. Weinert).

0022-328X/$ – see front matter © 2011 Elsevier B.V. All rights reserved.
doi:10.1016/j.jorganchem.2011.05.012

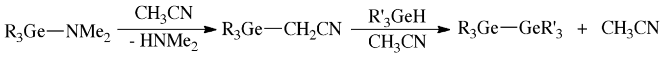

Scheme 1.

2. Results and discussion

The germane (*o*-Bu^{t}C$_6$H$_4$)$_3$GeBr (**1**) was synthesized starting from *o*-Bu^{t}C$_6$H$_4$NH$_2$, which was converted to the aryl bromide *o*-Bu^{t}C$_6$H$_4$Br via the Sandmeyer reaction and then to the corresponding Grignard reagent (*o*-Bu^{t}C$_6$H$_4$)MgBr. The Grignard reagent was then added to GeBr$_4$ in a 3:1 stoichiomeric ratio to furnish **1** (Scheme 2). Germanium(IV) bromide was used in lieu of the less expensive GeCl$_4$ to avoid obtaining mixed halide products, and the Grignard reagent was used instead of the organolithium reagent *o*-Bu^{t}C$_6$H$_4$Li since we have found that use of the latter type of alkylating agents results in the generation of a significant amount of polymeric material. Compound **1** has been characterized by NMR (^{1}H and ^{13}C) spectroscopy and elemental analysis. The protons of the *ortho-tert*-butyl group give rise to a singlet at δ 1.53 ppm in the ^{1}H NMR of **1** and resonances for the four aromatic protons were observed as the expected pattern of two doublets and two triplets.

We attempted to prepare the amide (*o*-Bu^{t}C$_6$H$_4$)$_3$GeNMe$_2$ from **1** by the metathesis reaction of **1** and LiNMe$_2$ in benzene or THF solvent, but both reactions were unsuccessful. However, **1** could be converted to the hydride species (*o*-Bu^{t}C$_6$H$_4$)$_3$GeH (**2**) upon treatment with lithium aluminum hydride in 93% yield (Scheme 3). The ^{1}H NMR spectrum of **2** exhibits a peak at δ 5.95 ppm corresponding to the Ge—*H* proton as well as a peak at δ 1.56 ppm for the protons of the *tert*-butyl group, and the IR spectrum of **2** contains a sharp band at 2083 cm^{-1} resulting from the stretching of the Ge—H bond. The attempted reaction of **2** with Ph$_3$GeNMe$_2$ in CH$_3$CN solvent at 85 °C was unsuccessful, as the hydride resonance for **2** remained present even after a reaction time of 96 h. Compound **2** was converted to the corresponding chloride compound (*o*-Bu^{t}C$_6$H$_4$)$_3$GeCl (**3**) by reluxing the hydride in benzene in the presence of CuCl$_2$ (Scheme 3) [11], and **3** was characterized by ^{1}H NMR spectroscopy and elemental analysis. The ^{1}H NMR spectrum of **3** is nearly identical to that of **1** and **2**, with a resonance at δ 1.52 ppm corresponding to the *o*-Bu^t group and four aromatic resonances for the protons attached to the phenyl rings. Although the salt metathesis reaction between **1** and LiNMe$_2$ was not successful, the reaction of **1** with KOH in refluxing absolute ethanol yielded the germanol (*o*-Bu^{t}C$_6$H$_4$)$_3$GeOH (**4**) in 77% yield (Scheme 3). The ^{1}H NMR spectrum of **4** contains a singlet at δ 1.51 ppm corresponding to the protons of the *tert*-butyl group as well as a broad singlet at δ 4.05 ppm that is assigned to the single proton of the —OH group.

In order to assess the steric environment about the central germanium atom, the X-ray structures of **1**–**4** were obtained, and

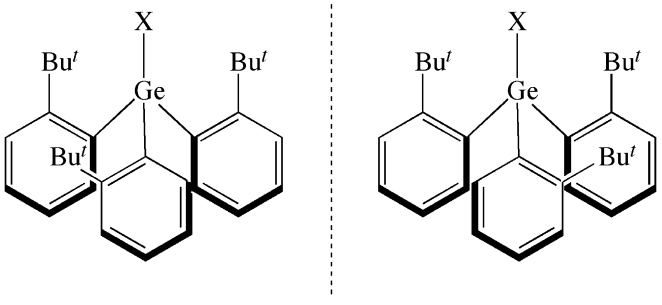

Fig. 1. Non-superimposable mirror images of *ortho-tert*-butylphenyl substituted germanes.

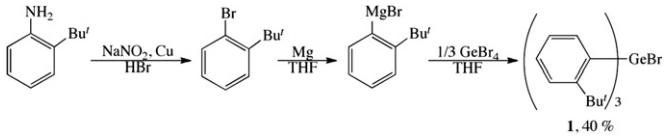

Scheme 2.

ORTEP diagrams are shown in Figs. 2–5 (respectively) while metric parameters are collected in Table 1. Compound **1** adopts a C_3-symmetric structure in the solid state (Fig. 2), with a Ge—C bond length of 1.997(2) Å and a Ge—Br bond distance of 2.362(1) Å (Table 1). The Ge—Br bond length compares to those in other related triaryl-susbstituted compounds, including Ph$_3$GeBr (**7**) [12], (*o*-(MeOCH$_2$)C$_6$H$_4$)$_3$GeBr (**8**) [13], and (*o*-(Bu^{t}O)$_2$C$_6$H$_3$)$_3$GeBr (**9**) [14], and relevant metric parameters for these three compounds are shown in Table 2. It also matches with the sum of the covalent radii of germanium and bromine of 2.35 Å [15]. The Ge—C distance in **1** is elongated from that of the typical Ge—C$_{ipso}$ bond length of 1.95 Å and also from the sum of the covalent radii of germanium and carbon (1.96 Å) [15] due to the presence of the bulky *ortho-tert*-butyl groups. The Ge—C bond distances in **1** are also elongated relative to the average Ge—C bond lengths in **7**, **8**, and **9**, due the steric effects of the *ortho-tert*-butyl groups. Compound **9** also contains a *tert*-butyl group, but the oxygen atom located between the tertiary carbon of the *tert*-butyl group and the *ortho*-carbon of the aryl ring diminishes the steric impact of the Bu^t-group.

The aryl rings in **1** are oriented such that each of the *tert*-butyl groups are pointed in the same direction as the Ge—Br bond. The orientation of the three aryl rings and the resulting disposition of the substituents limits access to the bromine in **1**. Despite the steric congestion, however, the bond angles about the central germanium atom do not differ significantly from the idealized tetrahedral angle of 109.5°. The C$_{ipso}$—Ge—C$_{ipso}$ bond angle in **1** is 108.26(6)° while the Br—Ge—C$_{ipso}$ bond is 110.66(6)°. This contrasts with the structures of **8** [13] and **9** [14], where the corresponding bond angles are distorted from the idealized tetrahedral geometry (Table 2).

The structure of **2** was obtained and is partially disordered with a molecule of the bromide **1** that occupies essentially the same volume as the hydride species and is present approximately 6% of the time. Additionally, there are two independent molecules of the hydride **2** in the unit cell, and the ORTEP diagram shown in Fig. 3 shows one of the two molecules. We made several attempts to obtain X-ray quality crystals of **2** that were not disordered in this fashion but were unsuccessful. Overall, the structure of **2** resembles that of the bromo-substituted derivative **1**. The average Ge—C bond length in **2** among the two independent molecules is 1.985(2) Å and the average C$_{ipso}$—Ge—C$_{ipso}$ angle is 108.05(8)°, both of which are also very similar to the corresponding values in **1** (Table 1). The hydrogen bound to germanium was refined, and the Ge—H bond distance is 1.37(2) Å.

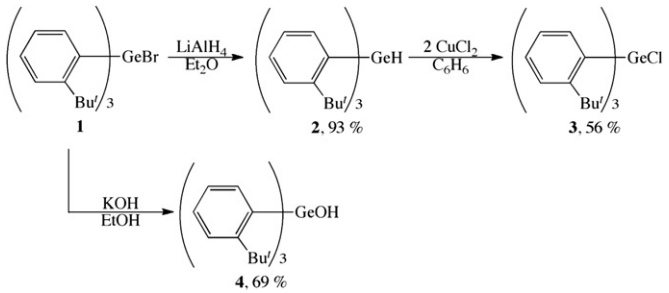

Scheme 3.

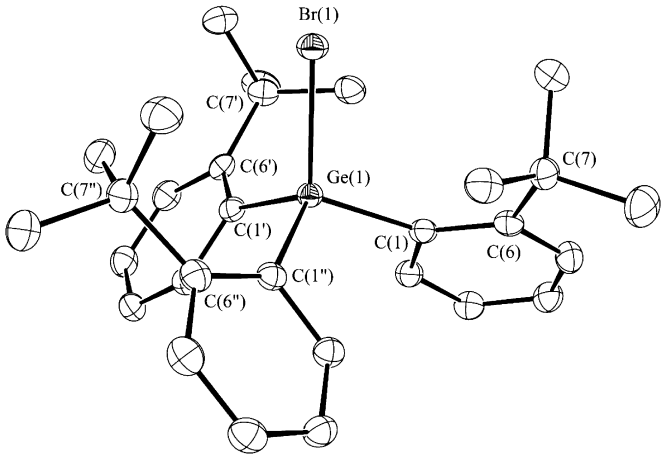

Fig. 2. ORTEP diagram of (*o*-Bu^{t}C$_6$H$_4$)$_3$GeBr (**1**). Thermal ellipsoids are drawn at 50% probability.

The structure of **2** can be compared to the arylgermanium hydride species Ph_3GeH (**10**) [9], (*o*-$CH_3C_6H_4$)$_3$GeH (**11**) [16], and Mes_3GeH (**12**) (Table 2) [17]. The average Ge–C bond distance in **2** is elongated relative to the average Ge–C bonds in both **10** [9], and **11** [16] but are shorter than that in **12** [17]. The Ge–H bond distance in **2** is similar to that in **10** (1.48(3) Å) [9] but shorter than the corresponding distance in **11** (1.712(1) Å) [16]. The average C_{ipso}–Ge–C_{ipso} angle in **2** is more acute than that in **10** but is more obtuse than that in **11** and nearly identical to that in **12**. The structures of **2**, **10**, **11**, and **12** are only slightly distorted from the ideal tetrahedral geometry, but the steric effects of two *ortho*-methyl groups in the mesityl-substituted compound **12** have a more significant impact on the Ge–C bond lengths than do the single *ortho*-Bu^t or *ortho*-Me groups in **2** and **11**.

The structure of **3** is disordered, and all of the carbon atoms except C(10) occupy one of two sites with 50% occupancy, and the ORTEP diagram shown in Fig. 4 shows one orientation of the aromatic rings. Taking into account the dirsorder, the average Ge–C_{ipso} bond is 1.990(4) Å and the Ge–Cl bond length 2.198(1) Å (Table 1), and the latter matches exactly with the sum of the covalent radii for germanium and chlorine (2.20 Å) [15]. The Ge–C distances in **1** and **3** are similar despite the presence of the smaller

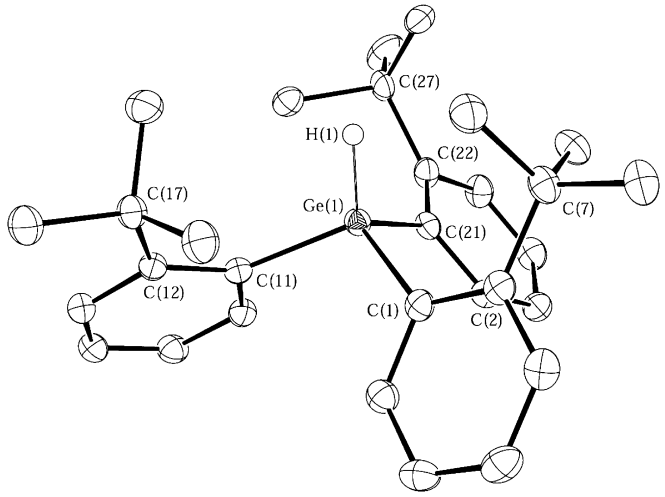

Fig. 3. ORTEP diagram of one molecule (molecule 1) of (*o*-Bu^{t}C$_6$H$_4$)$_3$GeH (**2**). Thermal ellipsoids are drawn at 50% probability.

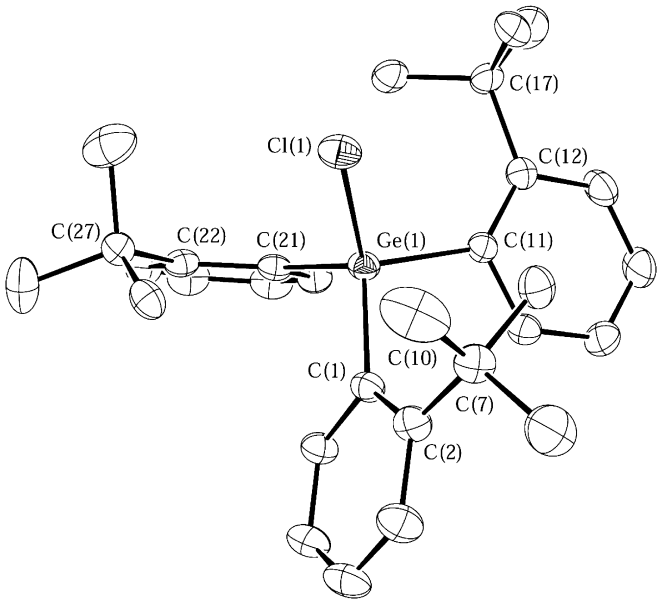

Fig. 4. ORTEP diagram of (*o*-Bu^{t}C$_6$H$_4$)$_3$GeCl (**3**). Thermal ellipsoids are drawn at 50% probability.

and more electronegative chlorine atom in **3** versus the bromine atom in **1**, and the aryl rings in both molecules of **3** are again oriented such that the *ortho-tert*-butyl substituents are disposed in the same direction as the Ge–Cl bonds. The geometry at the central germanium atom is nearly idealized tetrahedral in **3**, which has an average C_{ipso}–Ge–C_{ipso} bond angle of 108.8(2)° and an average C_{ipso}–Ge–Cl bond angle of 110.1(1)°. The geometry at germanium in **3** differs from those of the related species Ph_3GeCl (**13**) [18,19], (*o*-$(MeOCH_2)C_6H_4)_3$GeCl (**14**) [13], (*o*-$EtOC_6H_4)_3$GeCl (**15**) [20] (Table 2), where two different structures of **13** having different bond distances and angles have been reported. A comparison of these data indicates that among these four compounds, the structure of **3** most closely resembles the ideal tetrahedral structure expected for a germanium(IV) center.

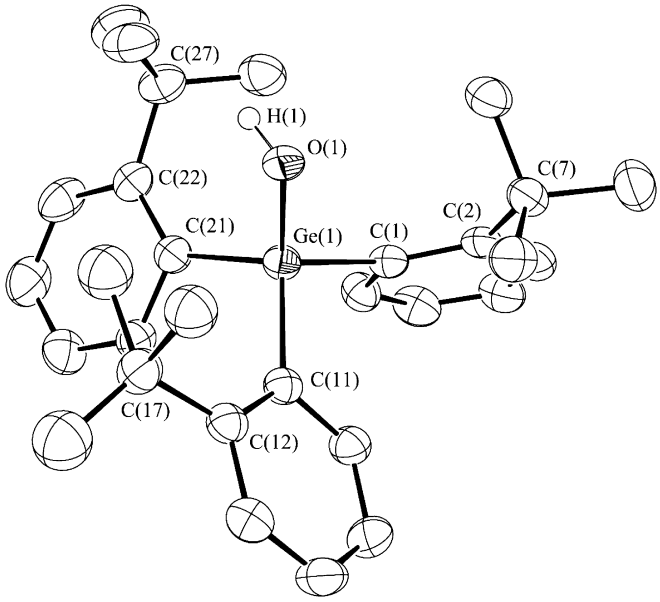

Fig. 5. ORTEP diagram of (*o*-Bu^{t}C$_6$H$_4$)$_3$GeOH (**4**). Thermal ellipsoids are drawn at 50% probability.

Table 1
Selected bond distances (Å) and angles (°) for **1**–**4**.

(o-Bu^{t}C$_6$H$_4$)$_3$GeBr (**1**)			
Ge(1)–Br(1)	2.362(1)	C(1)–Ge(1)–Br(1)	110.66(6)
Ge(1)–C(1)	1.997(2)	C(1)–Ge(1)–C(1′)	108.26(6)
(o-Bu^{t}C$_6$H$_4$)$_3$GeH (**2**)			
Molecule 1			
Ge(1)–C(1)	1.979(2)	C(1)–Ge(1)–C(11)	108.61(8)
Ge(1)–C(11)	1.985(2)	C(1)–Ge(1)–C(21)	106.85(8)
Ge(1)–C(21)	1.987(2)	C(11)–Ge(1)–C(21)	108.85(8)
Ge(1)–H(1)	1.37(2)	C(1)–Ge(1)–H(1)	111(1)
		C(11)–Ge(1)–H(1)	112(1)
		C(21)–Ge(1)–H(1)	110(1)
Molecule 2			
Ge(1′)–C(1′)	1.990(2)	C(1′)–Ge(1′)–C(11′)	107.54(8)
Ge(1′)–C(11′)	1.982(2)	C(1′)–Ge(1′)–C(21′)	108.53(8)
Ge(1′)–C(21′)	1.984(2)	C(11′)–Ge(1′)–C(21′)	107.91(8)
Ge(1′)–H(1′)	1.37(2)	C(1′)–Ge(1′)–H(1′)	110(1)
		C(11′)–Ge(1′)–H(1′)	109(1)
		C(21′)–Ge(1′)–H(1′)	114(1)
(o-Bu^{t}C$_6$H$_4$)$_3$GeCl (**3**)			
Ge(1)–Cl(1)	2.198(1)	C(1)–Ge(1)–C(11)	108.2(2)
Ge(1)–C(1)	1.975(4)	C(1)–Ge(1)–C(21)	110.3(2)
Ge(1)–C(11)	2.015(4)	C(11)–Ge(1)–C(21)	107.9(2)
Ge(1)–C(21)	1.979(4)	C(1)–Ge(1)–Cl(1)	109.6(1)
		C(11)–Ge(1)–Cl(1)	110.1(1)
		C(21)–Ge(1)–Cl(1)	110.6(1)
(o-Bu^{t}C$_6$H$_4$)$_3$GeOH (**4**)			
Ge(1)–O(1)	1.885(3)	C(1)–Ge(1)–C(11)	107.2(1)
Ge(1)–C(1)	1.991(3)	C(1)–Ge(1)–C(21)	108.0(1)
Ge(1)–C(11)	1.983(3)	C(11)–Ge(1)–C(21)	109.8(1)
Ge(1)–C(21)	1.976(4)	C(1)–Ge(1)–O(1)	113.5(1)
		C(11)–Ge(1)–O(1)	107.4(1)
		C(21)–Ge(1)–O(1)	110.9(1)

The structure of **4** (Fig. 5) again resembles those of **1**–**3**, where the *ortho*-*tert*-butyl groups are disposed in the same direction as the Ge–O bond and the average Ge–C bond length is 1.983(3) Å. The C_{ipso}–Ge–C_{ipso} angle in **4** is 108.3(1)° and the C_{ipso}–Ge–O angle is 110.6(1)°. The Ge–O bond distance is 1.885(3) Å, which is elongated relative to typical germanium–oxygen bonds that range from 1.76 to 1.84 Å in linear compopunds [21]. The structure of **4** can be compared to the unsubstituted derivative Ph_3GeOH [22] (**16**) as well as the sterically congested species Mes_3GeOH [23] (**17**) (Table 2). Compound **16** contains eight independent molecules in the unit cell [22], while **17** was obtained as a hydrogen bonded pair with Mes_3GeNCO. Among the three structures, the Ge–C and Ge–O bond lengths in **4** are longer than the corresponding distances in **16** and **17**, while the average C_{ipso}–Ge–C_{ipso} bond angle in **4** is the most acute and also the least distorted from the idealized tetrahedral bond angle. The C_{ipso}–Ge–O bond angle is more obtuse in **4** than in **16** or **17**, with the bond angle in **17** being the most acute. The hydroxide moiety in **17** is hydrogen bonded to the oxygen atom in Mes_3GeNCO, but no evidence for hydrogen bonding is present in the crystal structure of **4**. However, the infrared spectrum of **4** exhibits a broad band at 3356 cm^{-1}, indicating that some hydrogen bonding is present in the bulk material in nujoll mull.

The presence of the *ortho*-*tert*-butyl groups in **1**–**4** result in a distortion of the relative orientations of the aryl rings from the ideal geometry. In an ideal tetrahedral geometry, the dihedral angle between the plane of one aryl ring and that of each of the others would be 30°. These angles correspond to the angles between the Ge–C_{ipso} axis of one aryl ring and the C_{ipso}–C_{ortho} axis of the other aryl two rings, and therefore this corresponds to the C_{ipso}–Ge–C_{ipso}–C_{ortho} torsion angles within the molecule. In order to accommodate the three *ortho*-*tert*-butyl groups, the aryl rings are rotated such that one angle becomes more acute than 30° (α) and one becomes more obtuse than 30° (β) as shown in Fig. 6 [17,23]. With the exception of the C_3-symmetric **1**, these angles each occur three times in each molecule, and the values shown in Table 3 are the average of these three values for each molecule. This type of distortion is also observed in substituted aryl germanes where the *ortho*-substituents all point in the same direction, or in compounds that have two *ortho*-substituents, and so is also observed in Mes_3-GeH (**12**) [17] and Mes_3GeOH (**17**) [23]. The value of φ can then be used to describe the rotation of the rings in these species, where $\varphi = 1/2[(\alpha + 30°) + (\beta - 30°)]$.

The data shown in Table 3 indicate that **1**–**4** and **12** all have approximately the same amount of distortion from the idealized structure. The hydride species **2** is the most distorted among these molecules, with a φ value of 49.3°, and the hydroxide **4** also is significantly distorted with a φ value of 48.0°. The fourth substituent at germanium in **2** and **4** are the smallest among the four compounds **1**–**4** and these two species have the shortest Ge–C bond lengths. These data also indicate that the steric effects of one *ortho*-*tert*-butyl group are comparable to those of two *ortho*-methyl groups as the distortions of the five species **1**–**4** and **12** are similar. The *ortho*-tolyl substituted compound **11**, which has only one methyl group in the *ortho*-position, is significantly less distorted than the more sterically encumbered species **1**–**4** and **12**. Similarly, the di(*ortho*-*tert*-butoxy) substituted compound **9** is also less distorted than these five molecules since the oxygen atom in this species results in the six *tert*-butyl groups being disposed farther from one another than in **1**–**4**.

Table 2
Structural parameters for compounds **7**–**17**.

Compound	Ge–X bond length (Å)	Avg. Ge–C_{ipso} bond length (Å)	Avg. C_{ipso}–Ge–C_{ipso} bond angle (°)	Avg. C_{ipso}–Ge–X bond angle (°)	Ref.
Ph_3GeBr (**7**)	2.3188(7)	1.934(1)	112.44(1)	106.31(1)	[12]
(o-(MeOCH$_2$)C$_6$H$_4$)$_3$GeBr (**8**)	2.3617(5)	1.951(4)	114.7(2)	103.6(1)	[13]
(o-(Bu^{t}O)$_2$C$_6$H$_3$)$_3$GeBr (**9**)	2.3791(6)	1.965(2)	115.55(9)	102.38(6)	[14]
Ph_3GeH (**10**)[a]	1.48(3)	1.945(5)	110.2(1)	109(2)	[9]
(o-CH$_3$C$_6$H$_4$)$_3$GeH (**11**)	1.712(1)	1.981(1)	106.3(1)	112.69(1)	[16]
Mes_3GeH (**12**)	n/a	2.037(9)	108.9(4)	n/a	[17]
Ph_3GeCl (**13**)	2.187(2)	1.937(6)	112.5(2)	106.2(2)	[18]
Ph_3GeCl (**13**)	2.161(2)	1.933(5)	112.7(2)	106.0(1)	[19]
(o-(MeOCH$_2$)C$_6$H$_4$)$_3$GeCl (**14**)	2.213(1)	1.951(2)	115.3(1)	102.81(9)	[13]
(o-EtOC$_6$H$_4$)$_3$GeCl (**15**)	2.2287(8)	1.941(3)	112.6(1)	106.1(1)	[20]
Ph_3GeOH (**16**)	1.791(8)	1.93(2)	111.8(4)	107.1(4)	[22]
Mes_3GeOH (**17**)	1.805(3)	1.972(5)	114.7(2)	103.6(2)	[23]

[a] Values are for the average of two different morphologies.

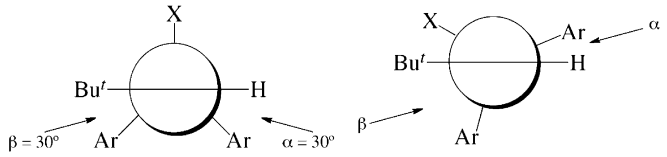

Fig. 6. Newman projections of *ortho-tert*-butylphenyl substituted germanes showing the idealized geometry (left) and distorted geometry (right).

The diaryl-substituted derivatives (*o*-Bu^{t}C$_6$H$_4$)$_2$GeBr$_2$ (**5**) and Mes$_2$GeH$_2$ (**6**) were also prepared and structurally characterized. Compound **5** was prepared in a similar manner to the method used for **1** using a 2:1 stoichiometric ratio of Grignard reagent to GeBr$_4$, while **6** was prepared according to the literature procedure [10]. The ^{1}H NMR of **5** is again similar to those of **1**–**4**, with a resonance at δ 1.54 ppm for the *ortho-tert*-butyl protons and four distinct aromatic resonances. The ^{1}H NMR of **6** matches that in the literature [10], with a resonance at δ 5.27 ppm corresponding to the hydrogen attached to the central germanium atom.

The ORTEP diagrams for **5** and **6** are shown in Figs. 7 and 8, and structural parameters are collected in Table 4. Compound **5** crystallizes with two independent molecules in the unit cell, and in both molecules the *ortho-tert*-butyl groups are directed away from the two Ge–Br bonds. The average Ge–C bond length among the two independent molecules is 1.965(6) Å while the average Ge–Br bond distance is 2.345(9) Å. Both of these distances are shorter than those in the corresponding triaryl species **1** due to an alleviation of the steric crowding at the germanium center in **5** since only two *ortho*-substituted aryl substituents are present. The average Br–Ge–Br, C$_{ipso}$–Ge–C$_{ipso}$, and Br–Ge–C$_{ipso}$ angles in **5** are 97.61(3), 130.4(3), and 106.1(2)° (respectively). The C–Ge–C bond angle at the central germanium atom in **5** is substantially more obtuse than that in **1**, and the absence of a third aryl substituent allows the two sterically encumbered aryl groups in **5** to be disposed farther away from one another.

The structure of **6** is C_2-symmetric, with a Ge–C bond distance of 1.965(2) Å and a C$_{ipso}$–Ge–C$_{ipso}$ bond angle of 113.2(1)°. The hydrogen atoms attached to germanium were found and refined, and the Ge–H bond distance is 1.43(3) Å, and the two C$_{ipso}$–Ge(1)–H(1) bond angles are 111(1) and 107(1)°. As expected, the absence of a third mesityl group in **6** versus the three mesityl groups present in **12** alleviates a significant amount of steric strain. The Ge–C bond length in **6** is shorter than the average distance in **12** (2.05(1) Å) by 0.08 Å and the C$_{ipso}$–Ge–C$_{ipso}$ bond angle in **6** is more obtuse than that in **12** (109.0(3)°) by 4.1°.

In conclusion, the four new *ortho-tert*-butylphenyl substituted germanes (*o*-Bu^{t}C$_6$H$_4$)$_3$GeX (X = Br (**1**), H (**2**), Cl (**3**), or OH (**4**)) have been prepared and structurally characterized. For the halide substituted species **1** and **3**, limited reactivity at the central Ge–X bond was observed, and these compounds could not be used to prepare the desired amide (*o*-Bu^{t}C$_6$H$_4$)$_3$GeNMe$_2$ for use in the hydrogermolysis reaction. Compound **2** was also found to be unreactive in the hydrogermolysis reaction with Ph$_3$GeNMe$_2$. The structures of **1**–**4** have been obtained and the *ortho-tert*-butyl substituents are oriented in the same direction as the Ge–X bond in each molecule. The presence of these substituents results in distortions in **1**–**4** from the ideal tetrahedral geometry. An assessment of the torsion angles within these four compounds indicates that the distortion is more significant in the hydride **2** and the hydroxide **4**, which contain the least sterically encumbering fourth substituent at germanium. The two diaryl-substituted germanes (*o*-Bu^{t}C$_6$H$_4$)$_2$GeBr$_2$ (**5**) and Mes$_2$GeH$_2$ (**6**) have also been prepared and structurally characterized, and a comparison of the structures of these two compounds versus their corresponding triaryl-substituted analogues (*o*-Bu^{t}C$_6$H$_4$)$_3$GeBr (**1**) and Mes$_3$GeH (**12**) indicate that the absence of a third sterically encumbering aryl group alleviates a significant amount of structural strain leading to shorter Ge–C$_{ipso}$ bond distances in **5** and **6**.

Table 3
Torsion angles and structural parameters for **1**–**4**, **9**, **11**, and **12**.

Compound	α (°)	β (°)	ϕ (°)
(*o*-Bu^{t}C$_6$H$_4$)$_3$GeBr (**1**)	14.8	74.3	44.5
(*o*-Bu^{t}C$_6$H$_4$)$_3$GeH (**2**)	18.0	80.6	49.3
(*o*-Bu^{t}C$_6$H$_4$)$_3$GeCl (**3**)	15.8	75.7	45.8
(*o*-Bu^{t}C$_6$H$_4$)$_3$GeOH (**4**)	17.5	78.5	48.0
(*o*-(Bu^{t}O)$_2$C$_6$H$_3$)$_3$GeBr (**9**) [14]	14.0	59.2	36.6
(*o*-CH$_3$C$_6$H$_4$)$_3$GeH (**11**) [16]	2.7	66.1	34.4
Mes$_3$GeH (**12**) [17]	3.0	81.8	42.4

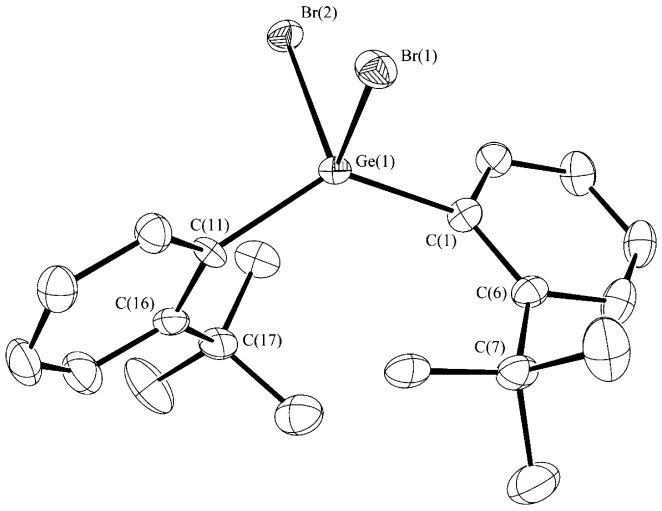

Fig. 7. ORTEP diagram of one molecule (molecule 1) of (*o*-Bu^{t}C$_6$H$_4$)$_2$GeBr$_2$ (**5**). Thermal ellipsoids are drawn at 50% probability.

3. Experimental

3.1. General considerations

All manipulations were carried out using standard Schlenk, syringe, and glovebox techniques [24]. The starting material *o*-Bu^{t}C$_6$H$_4$NH$_2$ was purchased from Aldrich and was distilled prior to use, and was converted to *o*-Bu^{t}C$_6$H$_4$Br via a literature method [25]. Germanium(IV) bromide was purchased from Gelest and anhydrous CuCl$_2$ was purchased from Fluka, and these reagents

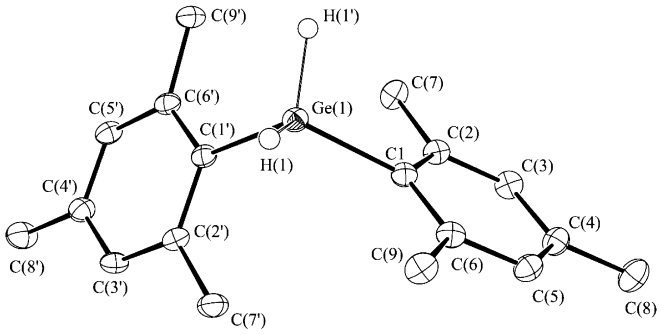

Fig. 8. ORTEP diagram of Mes$_2$GeH$_2$ (**6**). Thermal ellipsoids are drawn at 50% probability.

Table 4
Selected bond distances (Å) and angles (°) for **5** and **6**.

(o-Bu^{t}C$_6$H$_4$)$_2$GeBr$_2$ (**5**)			
Molecule 1			
Ge(1)–Br(1)	2.3497(9)	Br(1)–Ge(1)–Br(2)	96.14(3)
Ge(1)–Br(2)	2.3404(9)	Br(1)–Ge(1)–C(1)	103.7(2)
Ge(1)–C(1)	1.958(6)	Br(1)–Ge(1)–C(11)	110.1(2)
Ge(1)–C(11)	1.967(6)	Br(2)–Ge(1)–C(1)	109.1(2)
		Br(2)–Ge(1)–C(11)	104.9(2)
		C(1)–Ge(1)–C(11)	128.4(3)
Molecule 2			
Ge(1′)–Br(1′)	2.3486(9)	Br(1′)–Ge(1′)–Br(2′)	99.08(4)
Ge(1′)–Br(2′)	2.341(1)	Br(1′)–Ge(1′)–C(1′)	108.9(2)
Ge(1′)–C(1′)	1.969(6)	Br(1′) –Ge(1′)–C(11′)	101.3(2)
Ge(1′)–C(11′)	1.967(6)	Br(2′)–Ge(1′)–C(1′)	101.7(2)
		Br(2′)–Ge(1′)–C(11′)	109.1(2)
		C(1′)–Ge(1′)–C(11′)	132.3(3)
Mes$_2$GeH$_2$ (**6**)			
Ge(1)–C(1)	1.965(2)	C(1)–Ge(1)–C(1′)	113.2(1)
Ge(1)–H(1)	1.43(3)	C(1)–Ge(1)–H(1)	111(1)
		C(1′)–Ge(1)–H(1)	107(1)

were used without further purification. Compound **6** (Mes$_2$GeH$_2$) was prepared according to a literature procedure [10]. All solvents were purified using a Glass Contour solvent purification system. The NMR spectra (^{1}H and ^{13}C) were recorded using a Gemini 2000 NMR spectrometer and were referenced to residual protio solvent, and IR spectra were obtained using a Hewlett-Packard IR spectrometer. Elemental analyses were obtained by Midwest Microlabs (Indianapolis, IN) or Galbraith Laboratories (Knoxville, TN).

3.1.1. Synthesis of (o-Bu^{t}C$_6$H$_4$)$_3$GeBr (**1**)

A 15 mL aliquot of solution of o-Bu^{t}C$_6$H$_4$Br (10.60 g, 49.76 mmol) in THF (100 mL) was added to Mg metal (1.77 g, 72.8 mol) in a three-necked round bottom flask equipped with a reflux condenser and addition funnel and the reaction was initiated with a single crystal of I$_2$. The remaining solution was added dropwise to the flask and was subsequently refluxed for 90 min. After cooling to room temperature, the resulting solution was added to GeBr$_4$ (6.50 g, 16.6 mmol) in THF (50 mL) via cannula. The solution was refluxed under N$_2$ for 60 min, was cooled to room temperature, and was poured over 100 mL of aqueous HBr solution in an ice bath. The mixture was extracted with benzene (5 × 50 mL) in air, the organic phase was dried over MgSO$_4$, and the volatiles were removed *in vacuo* after gravity filtration to yield 3.7 g (40%) of **1** as a white solid. ^{1}H NMR (C$_6$D$_6$, 25 °C) δ 7.64 (d, J = 7.2 Hz, 3H, o-C$_6H_4$), 7.53 (d, J = 7.5 Hz, 3H, m-C$_6H_4$), 7.08 (t, J = 7.2 Hz, 3H, m-C$_6H_4$), 6.74 (t, J = 7.5 Hz, 3H, p-C$_6H_4$), 1.53 (s, 27H, –C(CH_3)$_3$) ppm. ^{13}C NMR (C$_6$D$_6$, 25 °C) δ 156.6 (Ge–C_{ipso}), 139.1 (o-CH), 137.0 (o-CBu^t), 130.8 (m-C),

Table 5
Crystallographic data for compounds **1**–**6**.

Compound	**1**	**2**	**3**	**4**	**5**	**6**
Empirical formula	$C_{30}H_{39}BrGe$	$C_{30}H_{40}Br_{0.03}Ge$	$C_{30}H_{39}ClGe$	$C_{30}H_{40}GeO$	$C_{20}H_{26}Br_2Ge$	$C_{18}H_{24}Ge$
Formula weight	552.11	475.61	507.65	489.21	498.82	312.96
Temperature (K)	100(2)	100(2)	100(2)	200(2)	150(2)	100(2)
Wavelength (Å)	0.71073	1.54184	0.71073	0.71073	0.71073	0.71073
Crystal system	Rhombohedral	Triclinic	Triclinic	Monoclinic	Triclinic	Monoclinic
Space group	*R*3	*P*-1	*P*-1	$P2_1/c$	*P*-1	$C2/c$
a, Å	11.247(3)	10.7792(6)	10.712(4)	13.584(2)	9.527(1)	13.298(3)
b, Å	11.247(3)	15.0437(8)	10.766(4)	17.852(2)	13.997(2)	9.040(2)
c, Å	38.28(2)	17.435(1)	14.495(6)	10.8475(2)	15.749(2)	13.426(3)
α, °	90	69.111(3)	111.577(4)	90	105.350(2)	90
β, °	90	88.715(3)	91.723(5)	91.425(5)	92.389(2)	102.752(4)
γ, °	120	76.374(3)	116.183(4)	90	98.993(2)	90
V, Å^3	4193(2)	2561.1(2)	1357.4(9)	2629.8(7)	1992.7(5)	1574.1(7)
Z	6	4	2	4	4	4
ρ (g cm^{-1})	1.312	1.233	1.242	1.236	1.663	1.321
Absorption coefficient (mm^{-1})	2.540	1.710	1.242	1.184	5.546	1.932
F(000)	1716	1012	536	1040	992	656
Crystal size (mm^3)	0.26 × 0.25 × 0.20	0.35 × 0.17 × 0.15	0.30 × 0.20 × 0.10	0.29 × 0.28 × 0.28	0.25 × 0.25 × 0.15	0.24 × 0.20 × 0.18
Theta range for data collection	1.60–28.03°	4.23–65.60°	1.55–28.65°	2.63–25.06°	1.35–25.43°	2.75–27.91°
Index ranges	$-14 \le h \le 14$ $-14 \le k \le 10$ $-46 \le l \le 49$	$-10 \le h \le 12$ $-17 \le k \le 17$ $-20 \le l \le 20$	$-14 \le h \le 14$ $-14 \le k \le 14$ $-18 \le l \le 18$	$-16 \le h \le 16$ $-20 \le k \le 21$ $-12 \le l \le 12$	$-11 \le h \le 11$ $-16 \le k \le 16$ $-18 \le l \le 18$	$-17 \le h \le 17$ $-11 \le k \le 11$ $-16 \le l \le 17$
Reflections collected	10,332	21,818	21,182	25,659	29,446	7069
Independent reflections	2150 (R_{int} = 0.0445)	8330 (R_{int} = 0.0340)	6121 (R_{int} = 0.0439)	4643 (R_{int} = 0.0576)	7270 (R_{int} = 0.0439)	1800 (R_{int} = 0.0371)
Completeness to θ	θ = 25.00 (100.0%)	θ = 60.00 (99.2%)	θ = 25.00 (98.1%)	θ = 25.00 (99.9%)	θ = 25.00 (99.3%)	θ = 25.00 (100.0%)
Absorption correction	Multi-scan/sadabs	Semi-empirical from equivalents	None	Multi-scan/sadabs	Multi-scan	Multi-scan/sadabs
Max. and min. transmission	0.6306 and 0.5581	0.7782 and 0.5779	0.8859 and 0.7070	0.7328 and 0.7253	0.4901 and 0.3378	0.7224 and 0.6542
Refinement method	Full-matrix least-squares on F^2	Full-matrix least-squares on F^2	Full-matrix least-squares on F^2	Full-matrix least-squares on F^2	Full-matrix least-squares on F^2	Full-matrix least-squares on F^2
Data/restraints/parameters	2150/0/100	8330/0/631	6121/0/566	4643/12/1293	7270/0/427	1800/0/94
Goodness-of-fit on F^2	1.014	1.028	1.043	1.044	1.076	1.077
Final R indices ($I < 2\sigma(I)$)						
R_1	0.0283	0.0323	0.0374	0.0435	0.0527	0.0290
wR_2	0.0659	0.0806	0.0842	0.1083	0.1555	0.0779
Final R indices (all data)						
R_1	0.0371	0.0384	0.0486	0.0736	0.0647	0.0306
wR_2	0.0699	0.0855	0.0911	0.1207	0.1630	0.0792
Largest diff. peak and hole (e Å^{-3})	0.414 and −0.745	0.567 and −0.390	0.808 and −0.587	0.669 and −0.416	3.080 and −1.136	1.085 and −0.640
CCDC deposition number	822221	822223	822222	822437	822220	822224

129.2 (*m*-C), 125.1 (*p*-C), 38.4 (-*C*(CH_3)$_3$), 33.8 (-C(CH_3)$_3$) ppm. Anal. Calcd. for $C_{30}H_{39}BrGe$: C, 65.24; H, 7.12. Found: C, 65.11; H, 7.25.

3.1.2. Synthesis of (*o*-Bu^tC_6H_4)$_3$GeH (**2**)

To a solution of **1** (1.00 g, 1.81 mmol) in Et_2O (40 mL) was added a suspension of $LiAlH_4$ (0.23 g, 6.1 mmol) in Et_2O (20 mL) via cannula at 0°C. The reaction mixture was stirred for 3 h at room temperature and then was quenched with deoxygenated deionized water. The organic phase was separated and dried over anhydrous $MgSO_4$. The suspension was filtered and the volatiles were removed *in vacuo* to yield 0.80 g (93%) of **2** as a white solid. ^{1}H NMR (C_6D_6, 25 °C): δ 7.66 (d, J = 7.8 Hz, 3H, *o*-C_6H_4), 7.56 (d, J = 7.8 Hz, 3H, *m*-C_6H_4), 7.12 (t, J = 7.8 Hz, 3H, *m*-C_6H_4), 6.76 (t, J = 7.2 Hz, 3H, *p*-C_6H_4), 5.95 (s, 1H, Ge–*H*), 1.56 (s, 27H, -C(CH_3)$_3$) ppm. ^{13}C NMR (C_6D_6, 25 °C): δ 156.4 (Ge–C_{ipso}), 138.8 (*o*-CH), 136.7 (*o*-CBu^t), 130.1 (*m*-C), 128.9 (*m*-C), 124.7 (*p*-C), 38.1 (-*C*(CH_3)$_3$), 33.5 (-C(*C*H_3)$_3$) ppm. IR (nujol mull): 2083 cm^{-1} (ν_{Ge-H}). Anal. Calcd. for $C_{30}H_{40}Ge$: C, 76.12; H, 8.52. Found: C, 75.93; H, 8.44.

3.1.3. Synthesis of (*o*-Bu^tC_6H_4)$_3$GeCl (**3**)

To a solution of **2** (1.00 g, 2.11 mmol) in benzene (40 mL) was added $CuCl_2$ (0.57 g, 4.2 mmol) and a crystal of CuI. The reaction mixture was refluxed under N_2 for 24 h, was allowed to cool, and was filtered through Celite. The volatiles were removed *in vacuo* to yield **3** (0.600 g, 56%) as a white solid. ^{1}H NMR (C_6D_6, 25 °C): δ 7.53 (d, J = 7.2 Hz, 3H, *o*-C_6H_4), 7.50 (d, J = 7.2 Hz, 3H, *m*-C_6H_4), 7.08 (t, J = 7.2 Hz, 3H, *m*-C_6H_4), 6.73 (t, J = 7.2 Hz, 3H, *p*-C_6H_4), 1.52 (s, 27H, -C(*C*H_3)$_3$) ppm. ^{13}C NMR (C_6D_6, 25 °C): δ 156.7 (Ge–C_{ipso}), 138.8 (*o*-*C*H), 138.3 (*o*-CBu^t), 130.4 (*m*-C), 128.9 (*m*-C), 125.1 (*p*-C), 38.2 (-*C*(CH_3)$_3$), 33.3 (-C(*C*H_3)$_3$) ppm. Anal. Calcd. for $C_{30}H_{39}ClGe$: C, 70.95. H, 7.75. Found: C, 70.79; H, 7.71.

3.1.4. Synthesis of (*o*-Bu^tC_6H_4)$_3$GeOH (**4**)

A solution of **1** (0.776 g, 1.41 mmol) in absolute ethanol (40 mL) was added to a solution of KOH (0.125 g, 2.23 mmol) in absolute ethanol (50 mL) under N_2. The reaction mixture was refluxed under N_2 for 24 h and the volatiles were removed *in vacuo*. Benzene (25 mL) was added to the resulting solid material and the mixture was agitated and subsequently filtered through Celite. The volatiles were removed *in vacuo* to yield **4** (0.478 g, 69%) as a white solid. ^{1}H NMR (C_6D_6, 25 °C): δ 7.63 (d, J = 7.2 Hz, 3H, *o*-C_6H_4), 7.52 (d, J = 7.2 Hz, 3H, *m*-C_6H_4), 7.11 (t, J = 7.2 Hz, 3H, *m*-C_6H_4), 6.82 (t, J = 7.2 Hz, 3H, *p*-C_6H_4), 4.05 (br s, 1H, -O*H*), 1.51 (s, 27H, -C(*C*H_3)$_3$) ppm. ^{13}C NMR (C_6D_6, 25 °C): δ 156.9 (Ge–C_{ipso}), 139.1 (*o*-*C*H), 138.6 (*o*-CBu^t), 130.2 (*m*-C), 129.3 (*m*-C), 125.4 (*p*-C), 38.3 (-*C*(CH_3)$_3$), 33.7 (-C(*C*H_3)$_3$) ppm. IR (nujol mull): 3356 cm^{-1} (br, ν_{O-H}). Anal. Calcd. for $C_{30}H_{40}GeO$: C, 73.63; H, 8.24. Found: C, 73.48; H, 8.18.

3.1.5. Synthesis of (*o*-Bu^tC_6H_4)$_2$GeBr$_2$ (**5**)

A 15 mL aliquot of solution of *o*-Bu^tC_6H_4Br (7.73 g, 36.3 mmol) in THF (60 mL) was added was to Mg metal (1.32 g, 54.3 mol) in a three-necked round bottom flask equipped with a reflux condenser and addition funnel and the reaction was initiated with a single crystal of I_2. The remaining solution was added dropwise to the flask and was subsequently refluxed for 90 min. After cooling to room temperature, the resulting solution was added to $GeBr_4$ (7.12 g, 18.1 mmol) in THF (40 mL) via cannula. The solution was refluxed under N_2 for 90 min, was cooled to room temperature, and was poured over 100 mL of aqueous HBr solution in an ice bath. The mixture was extracted with benzene (5 × 50 mL) in air, the organic phase was dried over $MgSO_4$, and the volatiles were removed *in vacuo* after gravity filtration to yield 6.30 g (70%) of **5** as a white solid. ^{1}H NMR (C_6D_6, 25 °C) δ 7.64 (d, J = 7.2 Hz, 2H, *o*-C_6H_4), 7.54 (d, J = 7.8 Hz, 2H, *m*-C_6H_4), 7.09 (t, J = 7.8 Hz, 2H, *m*-C_6H_4), 6.74 (t, J = 7.2 Hz, 2H, *p*-C_6H_4), 1.54 (s, 18H, -C(*C*H_3)$_3$) ppm. ^{13}C NMR (C_6D_6, 25 °C) δ 156.6 (Ge–C_{ipso}), 139.1 (*o*-*C*H), 137.0 (*o*-CBu^t), 130.4 (*m*-C), 129.2 (*m*-C), 125.0 (*p*-C), 38.4 (-*C*(CH_3)$_3$), 33.8 (-C(*C*H_3)$_3$) ppm. Anal. Calcd. for $C_{20}H_{26}Br_2Ge$: C, 48.13; H, 5.25. Found: C, 47.92; H, 5.13.

3.2. X-ray structure analysis

X-ray crystallographic measurements for **1**–**4** and **6** were made using a Bruker APEX CCD system under a stream of nitrogen gas. Data were corrected for absorption using SADABS and the structures were solved using direct methods (SIR-2004). All non-hydrogen atoms were refined anisotropically by full-matrix least squares (SHELXL-97). The structure of **5** was acquired using a Bruker SMART X2S benchtop crystallographic system, using APEX2 software for the unit cell determination. Data were corrected from absorption using SADABS and all non-hydrogen atoms were refined using full-matrix least squares (SHELXL-2008). Crystallographic data for **1**–**6** are collected in Table 5.

Appendix A. Supplementary material

CCDC 822220–822224 and 822437 contains the supplementary crystallographic data for this paper. These data can be obtained free of charge from The Cambridge Crystallographic Data Centre via www.ccdc.cam.ac.uk/data_request/cif.

References

[1] E. Subashi, A.L. Rheingold, C.S. Weinert, Organometallics 25 (2006) 3211–3219.
[2] M.L. Amadoruge, A.G. DiPasquale, A.L. Rheingold, C.S. Weinert, J. Organomet. Chem. 693 (2008) 1771–1778.
[3] M.L. Amadoruge, J.R. Gardinier, C.S. Weinert, Organometallics 27 (2008) 3753–3760.
[4] M.L. Amadoruge, J.A. Golen, A.L. Rheingold, C.S. Weinert, Organometallics 27 (2008) 1979–1984.
[5] M.L. Amadoruge, E.K. Short, C. Moore, A.L. Rheingold, C.S. Weinert, J. Organomet. Chem. 695 (2010) 1813–1823.
[6] M.L. Amadoruge, C.S. Weinert, Chem. Rev. 108 (2008) 4253–4294.
[7] M.L. Amadoruge, C.H. Yoder, J.H. Conneywerdy, K. Heroux, A.L. Rheingold, C.S. Weinert, Organometallics 28 (2009) 3067–3073.
[8] C.S. Weinert, Dalton Trans. (2009) 1691–1699.
[9] G.S. McGrady, M. Odlyha, P.D. Prince, J.W. Steed, Cryst, Eng. Commun. 4 (2002) 271–276.
[10] J.A. Cooke, C.E. Dixon, M.R. Netherton, G.M. Kollegger, K.M. Baines, Synth. React. Inorg. Met. Org. Chem. 26 (1996) 1205–1217.
[11] J. Ohshita, Y. Toyoshima, A. Iwata, H. Tang, A. Kunai, Chem. Lett. 30 (2001) 886–887.
[12] H. Preut, F. Huber, Acta Cryst. B35 (1979) 83–86.
[13] Y. Sugiyama, T. Matsumoto, H. Yamamoto, M. Nishikawa, M. Kinoshita, T. Takei, W. Mori, Y. Takeuchi, Tetrahedron 59 (2003) 8689–8696.
[14] A. Schnepf, C. Drost, Dalton Trans. (2005) 3277–3280.
[15] P. Pyykkö, M. Atsumi, Chem. Eur. J. 15 (2009) 186–197.
[16] T.S. Cameron, K.M. Mannan, S.R. Stobart, Cryst. Struct. Commun. 4 (1975) 601–604.
[17] J.B. Lambert, C.L. Stern, Y. Zhao, W.C. Tse, C.E. Shawl, K.T. Lentz, L. Kania, J. Organomet. Chem. 568 (1998) 21–31.
[18] D. Dakternieks, A.E.K. Lim, B. Zobel, E.R.T. Tiekink, Main Group Met. Chem. 23 (2000) 789–790.
[19] P.D. Prince, G.S. McGrady, J.W. Steed, New J. Chem. 26 (2002) 457–461.
[20] C. Schaeffer, C. Yoder, A.L. Rheingold, CCDC 652595 (2007).
[21] K.M. Baines, W.G. Stibbs, Coord. Chem. Rev. 145 (1995) 157–200.
[22] G. Ferguson, J.F. Gallagher, D. Murphy, T.R. Spalding, C. Glidewell, H.D. Holden, Acta Cryst. C48 (1992) 1228–1231.
[23] G. Hihara, R.C. Hynes, A.-M. Lebuis, M. Rivière-Baudet, I. Wharf, M. Onyszchuk, J. Organomet. Chem. 598 (2000) 276–285.
[24] D.F. Shriver, M.A. Drezdzon, in: The Manipulation of Air Sensitive Compounds, second ed. John Wiley and Sons, New York, 1986.
[25] A. Mazzanti, L. Lunazzi, M. Minzoni, J.E. Anderson, J. Organomet. Chem. 71 (2006) 5474–5481.